Zeitschrift: Helvetica Physica Acta
Band: 53 (1980)
Heft: 2

Artikel: Reflectivity of bent quartz crystal plates
Autor: Dousse, J.-Cl. / Kern, J.
DOI: https://doi.org/10.5169/seals-115116

Helvetica Physica Acta, Vol. 53 (1980), Birkhäuser Verlag, Basel

Reflectivity of bent quartz crystal plates[1])

by **J. -Cl. Dousse and J. Kern**

Physics Department, University, CH-1700 Fribourg, Switzerland

(14. IV. 1980)

Abstract. The integrated reflectivities of a 2.5 mm and of a 6 mm thick quartz crystal plate have been measured with a DuMond spectrometer as a function of photon energy in the range 60 to 300 keV and for several diffraction orders. The bending radius was 5 m and the plates cut in such a way that the Miller indices of the reflecting planes were (110). The results are compared with predictions of the diffraction theory for mosaic crystals. The relevance and interpretation of this concept for quartz is discussed. It is shown that in order to reproduce the results, the model has to be modified to allow unequal mosaicity parameters along and across the plate. Primary and secondary extinction coefficients are deduced.

1. Introduction

The high precision and resolution of crystal spectrometers are obtained at the expense of a low luminosity compared to that of ionization detectors. A large crystal reflectivity is consequently of great importance. Quartz is one of the best crystals for use in such a spectrometer, since nearly perfect specimens of large size are available. The (110) reflecting planes obtained in a Y-cut are especially attractive since they are not deformed under bending by the Sumbayev effect [1]. In addition, reflexes can be observed up to high orders [2]. It can be shown [3] that the reflectivity of these planes is enhanced by subjecting the plate to static or alternating electric fields. Before explaining these new phenomena, it is appropriate to investigate how the current theories (see Section 2) apply to the zero-field situation. The validity of a mosaic model for quartz is discussed. In Section 3 we report on reflectivity measurements performed with a DuMond curved crystal spectrometer [4] of the transmission-type entailing Laue diffraction. It is then shown (Section 4 & 5) that for first-order reflections, the experimental results can be reproduced using kinematical theory corrected for primary and secondary extinction. For higher diffraction orders a modification of the model is required (Section 6).

2. Diffraction models

The first treatment of crystal diffraction was geometrical and is called the kinematical theory. In this model, interactions between incident and scattered

[1]) Work supported by the Swiss National Science Foundation

radiation fields are neglected. It is applicable to a thin perfect crystal. In the Laue case, the integrated reflectivity is given by [5]

$$R_{\text{kin}} = Q \cdot t_\theta \cdot \exp(-\mu_0 t_\theta) \tag{1}$$

where

$Q = (F \cdot N \cdot r_0)^2 \cdot \lambda^3 / \sin 2\theta$
F = structure factor
N = number of atoms per unit volume
r_0 = classical radius of the electron
λ = wavelength of diffracted photons
θ = Bragg angle
$t_\theta = t/\cos\theta$ where t is the plate thickness
μ_0 = linear absorption coefficient.

The aforementioned interaction is taken into account in the dynamical theory valid for large perfect crystals. The predicted integrated reflectivity for a thick but weakly absorbing crystal plate is then given by [6]

$$R_{\text{dyn}} = \tfrac{1}{2} \cdot (F \cdot N \cdot r_0 \cdot \lambda^2 / \sin 2\theta) \cdot \exp(-\mu_0 t_0) \tag{2}$$

In formulae (1) and (2) the Debye–Waller factor, which accounts for the thermal oscillation of the lattice points, has been omitted. This correction is unnecessary for our experimental conditions [7]. The polarization factors, which are nearly equal to unity have also been neglected.

It appears experimentally that in real crystals reflectivities are intermediate between the values predicted by the two theories. Darwin suspected that the mathematical lattice perfection assumed in the dynamical theory was not realized in large crystal pieces. He proposed the concept of a mosaic crystal consisting of small perfect regions, or crystallites, that are distributed in orientation over a small angle range. The kinematical theory applies provided the crystallite size is very small, and their distribution wider than the angular range of reflection of a single block. When the size of the crystallites is larger, so that primary extinction is no longer negligible, Darwin has shown [8] [9] that Q has to be replaced in (1) by Q' defined as

$$Q' = Q \cdot f(A_m) \tag{3}$$

where

$$A_m = F \cdot N \cdot r_0 \cdot \lambda \cdot [(1+\cos 2\theta)/2] \cdot t_m/\cos\theta \tag{3a}$$

t_m = average thickness of the crystallites.

For Laue diffraction, the function $f(A_m)$ is given by [6]

$$f(A_m) = \frac{\sum_{k=0}^{\infty} J_{2k+1}(2A_m) + \cos 2\theta \sum_{k=0}^{\infty} J_{2k+1}(2A_m \cos 2\theta)}{A_m(1+\cos 2\theta)} \tag{4}$$

where $J_{2k+1}(2A_m)$ is a Bessel function of order $(2k+1)$.

An additional phenomenon, called secondary extinction, results from the attenuation of the radiation reaching any block by the presence of preceding

crystallites with nearly parallel orientation. This decrease in intensity can be accounted for by using an effective attenuation coefficient μ in equation (1)

$$\mu = \mu_0 + g \cdot Q' \tag{5}$$

where g is a parameter which depends on the width (FWHM) ω of the crystallite angular distribution by the relation [6]

$$g = [(2 \cdot \ln 2)/\pi]^{1/2} \cdot \omega^{-1} \tag{6}$$

and where Q' is given by (3). It has been found experimentally that some crystals exhibit a real mosaic structure, with physically distinguishable blocks, although usually larger than those supposed by Darwin [10]. In topographic studies of high quality plates similar to those we are using for γ-ray spectroscopy, quartz appears to be a slowly varying perfect crystal [11]. Thus, like most crystals, quartz does not display a mosaic structure. This condition does not however need to be fullfilled to successfully apply Darwin's modified kinematical theory. We interpret this apparent contradiction as follows: the crystallite concept gives only a statistical description of the crystal behaviour. The blocks represent only a mathematical division of a nearly continuous structure, just as a distribution is divided in classes or a continuous curve approximated by a number of linear segments. In this way, the crystallite dimension t_m does not represent the average size of a physical object, but indicates the distance over which the lattice orientation changes by some angle. It is thus not necessarily a constant but could depend on various parameters, such as photon energy. For simplification, we will disregard these dependencies.

The formula we propose to use has been derived for unstrained crystals. The effect of bending has been considered by a number of authors, e.g. Despujols [12], for perfect crystals. Since the large plates we use do not have this quality, we have not followed this approach. In addition, the theory of X-ray diffraction to elastically bent perfect crystals gives results that tend to the mosaic limit for integrated reflectivity if the bending radius is made small enough [13]. We will propose in Section 6 a phenomenological modification of the model which takes into account the crystal curvature and/or the bending imperfections.

3. Experimental method

We have observed the reflectivity of two plates of thickness 2.5 mm and 6 mm respectively. The bending radius was 5 m and photons were diffracted by the (110) planes. The geometry is shown in Fig. 1. Radiation came from a ^{169}Yb radioactive source obtained by thermal neutron irradiation of ^{168}Yb enriched oxide. The source thickness was 0.05 mm, corresponding to an apparent angular width of 2 arcsec. A 33 cm^3 Ge(Li) detector and a 4000 channel analyzer were used for photon detection. For a given photon energy and order of reflection, the integrated reflectivity has been obtained by the following procedure:

(i) The spectrometer is set initially at angle zero (direct transmission case). The number of events per unit time is then observed in a given channel range selected to correspond to the transition of interest. After correction for dead time and background, the number n_0 of incident photons is obtained.

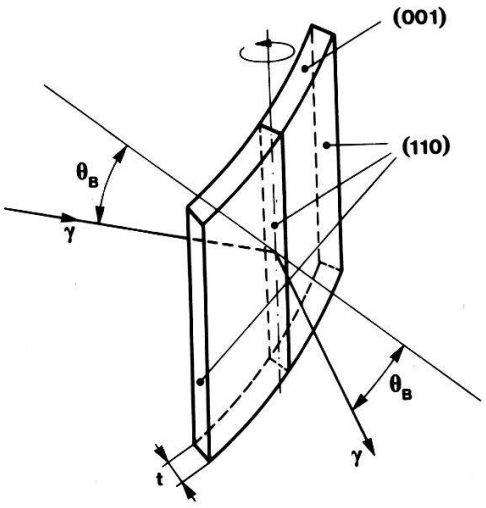

Figure 1
Geometrical arrangement.

(ii) The Bragg reflex corresponding to the same line is then observed point by point using an identical channel range. For every point, the numbers of counts are added. After correction for background, this sum divided by the total measuring time yields the number n of diffracted photons. The integrated reflectivity is then given by

$$R_{\text{obs}} = (n/n_0)\delta\theta \tag{7}$$

where $\delta\theta$ is the angular distance between two points.

Since the linear absorption is very nearly the same in the determination of n_0 and n, the factor $\exp(-\mu_0 t_\theta)$ does not need to be considered. In Table 1 are presented the experimental reflectivities obtained for the 2.5 mm plate and, for comparison, the corresponding theoretical values computed from expressions (1) and (2). It is apparent that the experiment values are intermediate between the two theoretical predictions. It is concluded that, as anticipated, the primary and secondary extinction phenomena cannot be neglected.

4. Evalution of the extinction parameters

Our purpose is to find out if the observed reflectivities can be described by a kinematical theory corrected for primary and secondary extinction. The problem is to determine t_m and g so that

$$R_{\text{obs}} = Q \cdot f(A_m) \cdot t_\theta \cdot \exp[-g \cdot Q \cdot f(A_m) \cdot t_\theta] \tag{8}$$

Table 1
Theoretical and experimental integrated reflectivities for the (110) planes of a 2.5 mm quartz plate. Order of reflection $n = 1$ ($F = 20.03$).

E[keV]	63.12	93.62	109.77	130.51	177.18	197.97	261.05	307.68
$R_{\text{dyn}}10^6$	1.20	0.81	0.69	0.53	0.43	0.38	0.29	0.25
$R_{\text{kin}}10^6$	58.98	26.83	19.52	13.81	7.50	6.01	3.45	2.49
$R_{\text{obs}}10^6$	2.83	2.25	2.10	1.80	1.45	1.29	1.03	0.92

A mathematical difficulty arises from the fact that t_m appears only implicitly in (8). In addition, as shown in Figure 2, $f(A_m)$ is not linear in t_m so that $\bar{f}(A_m)$ is not equal to $f(\bar{A}_m)$. We define $W(t_m)$ as the distribution of the crystallite sizes. The average primary extinction is then given by

$$\bar{f}(A_m) = \int f(A_m) \cdot W(t_m) \cdot dt_m \quad \text{where} \quad \int W(t_m) \cdot dt_m = 1 \tag{9}$$

Figure 3 shows that the shape of the distribution does not strongly influence the results. It shows also that the function $\bar{f}(A_m)$ becomes smoother with the increase of the distribution width. With regard to the above remarks, the following iterative procedure has been used to determine g and t_m:

(a) For an (arbitrary) initial value t_m, the average primary extinction $\bar{f}_i(A_m)$ is computed for each of the transition energies E_i, assuming for $W(t_m)$ a gaussian distribution of variance $\sigma = t_m/3$.

(b) The related quantity $\bar{Q}_i' t_\theta = Q_i \bar{f}_i(A_m) t_\theta$ is introduced in expression (8). This gives

$$g_i = (\bar{Q}_i' t_\theta)^{-1} \cdot \ln[(\bar{Q}_i' t_\theta)/R_{\text{obs}}(E_i)] \tag{10}$$

(c) The average value $\bar{g}$ is used to calculate the theoretical integrated reflectivities

$$R_{\text{th}}(E_i) = \bar{Q}_i' \cdot t_\theta \cdot \exp(-\bar{g} \cdot \bar{Q}_i' \cdot t_\theta) \tag{11}$$

(d) The quantities given by (11) are then compared to the experimental values. The main deviation $\overline{\Delta R}$ is defined as

$$\overline{\Delta R} = \frac{1}{n} \sum_{i=1}^{n} p_i \, |R_{\text{obs}}(E_i) - R_{\text{th}}(E_i)| \tag{12}$$

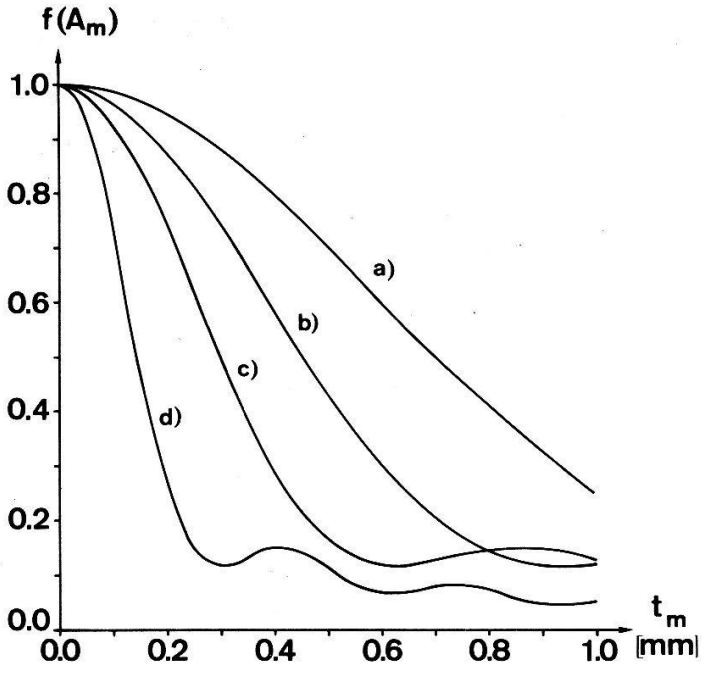

Figure 2
Variation of the primary extinction $f(A_m)$ as a function of t_m, the crystallite linear dimension, for the following photon energies:
a) 307.68 keV b) 197.97 keV c) 130.51 keV d) 63.12 keV.

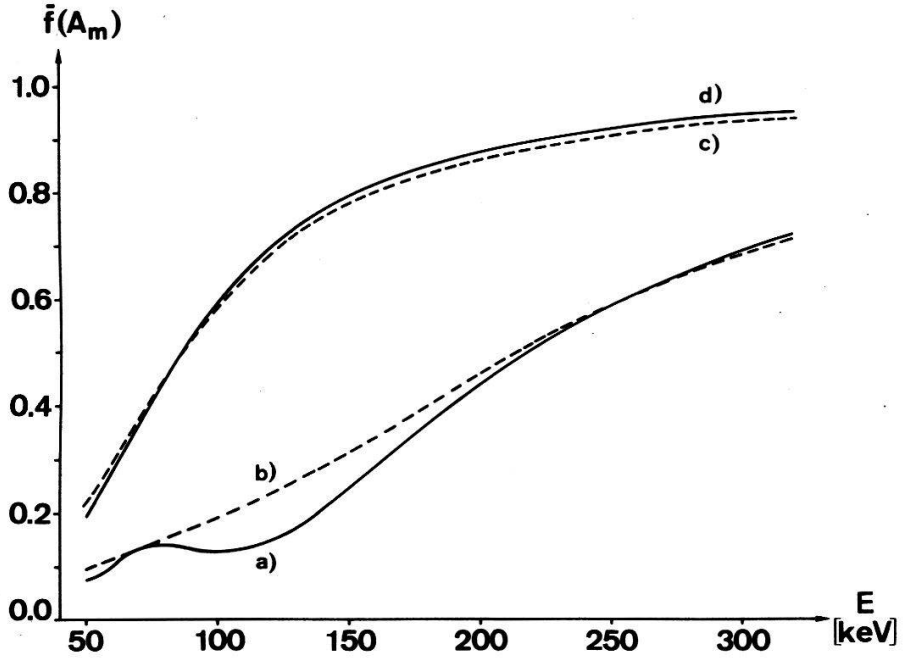

Figure 3
Dependence of the average primary extinction $\bar{f}(A_m)$ on the photon energy for different gaussian distributions $W(t_m)$ based on several crystallite sizes:
a) $t_m = 0.5$ mm, $\sigma = 0.06$ mm b) $t_m = 0.5$ mm, $\sigma = 0.18$ mm
c) $t_m = 0.2$ mm, $\sigma = 0.06$ mm or d) for a rectangular distribution of width equal to that of gaussian c).

where p_i is a weighing factor proportional to the experimental error on $R_{obs}(E_i)$.

(e) The procedure is then repeated, varying the parameter t_m and searching for a minimum value of $\overline{\Delta R}$.

It is interesting to note that when this condition is satisfied, the parameters g_i tend to be all approximately equal to $\bar{g}$ so that relation (10) can be written

$$\ln\left[(\bar{Q}_i' t_\theta)/R_{obs}(E_i)\right] = \bar{g} \cdot (\bar{Q}_i' t_\theta) \tag{13}$$

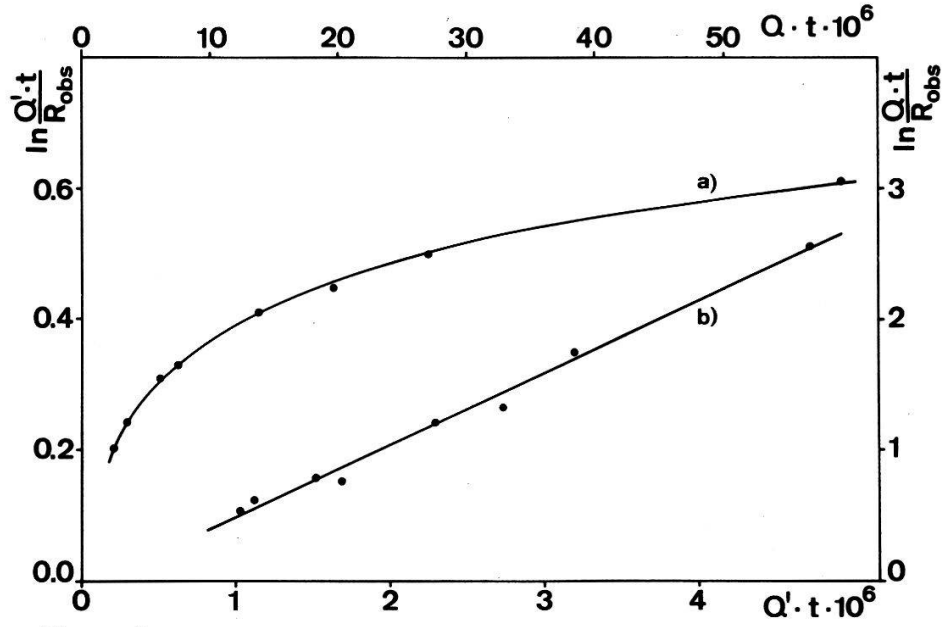

Figure 4
Plot of $\ln[Q't)/R_{obs}]$ as a function of $Q't$ $(t \simeq t_\theta)$ for a) $t_m = 0$ $(Q' = Q)$ b) $t_m = 0.87$ mm.

A plot of the expression on the left in (13) as a function of $(\bar{Q}'_i t_\theta)$ gives therefore a straight line with slope $\bar{g}$. If t_m is incorrectly chosen, the above graph is no longer straight: a curve of negative concavity is obtained for too small values of t_m and of positive concavity if t_m is too large. Figure 4 illustrates this situation.

5. Results for the first order of diffraction

Using the previously described method, we have obtained for the 2.5 mm plate the results reported in Table 2. It can be seen that the differences between measured and theoretical values are all smaller than the experimental errors. The relatively large value found for t_m implies a large primary extinction and explains the observed relatively low reflectivities. Replacing the value of $\bar{g} = 10.7 \cdot 10^4$ in relation (6), we find a mosaic width of 1.3 arcsec. This value is quite reasonable when compared to the observed width of the reflexes (3.5 arcsec) since the latter results also from the apparent source width (2 arcsec) and from imperfect crystal curvature.

6. Results at higher diffraction orders. Modification of the model

The next question is whether or not the parameters can reproduce the integrated reflectivities of a second and thicker plate cut from the same single crystal, and to investigate their validity for diffraction at several reflection orders. The same transitions from the ^{169}Yb decay have been observed with a 6 mm thick quartz plate in 1st, 2nd and 3rd order. Parameters t_m and $\bar{g}$ were fitted for each order using the method described in Section 4. The value of t_m decreased systematically with the diffraction order. This result is not at variance with our interpretation of the block concept, but the results were inferior to those obtained with the first plate, the average deviation $\overline{\Delta R}$ being about 5 to 10 times larger. It was then hypothesized that bending causes different linear dimensions across the plate (t_m) and perpendicular to the diffraction planes (t_t). Changes in the transverse dimension t_t affect the primary extinction coefficient, which depends on the number of planes intersected by the incident beam. In the standard model, this number is

$$m = (t_m \cdot \tan \theta_n)/d_{110} \tag{14}$$

Table 2
Theoretical ($t_m = 0.87$ mm, $\bar{g} = 10.7 \cdot 10^4$) and experimental integrated reflectivities for the planes (110) of the 2.5 mm quartz plate. Order of reflection $n = 1$.

E[keV]	$\bar{f}(A_m)$	$\exp(-\bar{g}\ \bar{Q}'t_\theta)$	$R_{th} \cdot 10^6$	$R_{obs} \cdot 10^6$
63.12	0.080	0.603	2.84	2.83±0.15
93.62	0.119	0.711	2.27	2.25±0.21
109.77	0.140	0.746	2.04	2.10±0.11
130.51	0.166	0.782	1.79	1.80±0.09
177.18	0.225	0.835	1.40	1.45±0.06
197.97	0.251	0.851	1.28	1.29±0.05
261.05	0.338	0.883	1.02	1.03±0.08
307.68	0.410	0.897	0.91	0.92±0.06

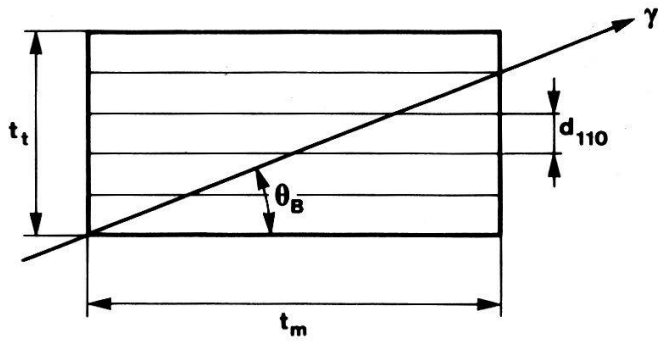

Figure 5
Orientation and dimensions of the crystallites.

where θ_n is the Bragg angle for the nth diffraction order and d_{110} the interplanar spacing.

As shown in Fig. 5, relation (14) is valid only if $t_m \tan \theta_n$ is smaller than t_t. Due to its $\tan \theta_n$ dependence, this condition is not satisfied for large n/E ratios. This explains the difficulties encountered with the observed reflectivities at low energies for diffraction orders $n = 2$ and $n = 3$. To take the new parameter t_t into account, the iterative procedure described in Section 4 was modified to vary t_t. For each pair of values (t_m, t_t), the validity of relation (14) is tested. If it is invalid, t_m is replaced in the computation of A_m by t'_m, where

$$t'_m = t_t/\tan \theta_n \tag{15}$$

The best values for t_m, t_t and $\bar{g}$ are given in Table 3 and the corresponding calculated reflectivities are compared with the experimental results in Table 4, 5 and 6. The agreement is very satisfactory.

Table 3
Fitted values of the extinction parameters for the 6 mm thick quartz plate.

n	t_m [mm]	t_t [mm]	$\bar{g} \cdot 10^{-4}$
1	0.64	0.022	7.79
2	0.48	0.017	7.97
3	0.68	0.022	11.46

Table 4
Theoretical and experimental integrated reflectivities for the (110) planes of a 6 mm quartz plate. Order of reflection $n = 1$ ($F = 20.03$).

E[keV]	$\bar{f}(A_m)$	$\exp(-\bar{g} \cdot \bar{Q}' t_\theta)$	$R_{th} \cdot 10^6$	$R_{obs} \cdot 10^6$
63.12	0.140	0.214	4.24	4.24±0.21
93.62	0.172	0.422	4.67	4.63±0.25
109.77	0.199	0.484	4.51	4.51±0.20
130.51	0.235	0.545	4.25	4.27±0.21
177.18	0.318	0.640	3.66	3.84±0.17
197.97	0.458	0.669	3.45	3.60±0.15
261.05	0.476	0.735	2.94	2.83±0.14
307.68	0.572	0.766	2.61	2.49±0.13

Table 5
Order of reflection $n = 2$ ($F = 21.74$).

E[keV]	$\bar{f}(A_m)$	$\exp(-\bar{g} \cdot \bar{Q}' t_\theta)$	$R_{th} \cdot 10^6$	$R_{obs} \cdot 10^6$
63.12	0.300	0.138	3.43	3.48±0.19
109.77	0.296	0.522	4.26	4.23±0.20
130.51	0.295	0.632	3.64	3.68±0.18
177.18	0.390	0.720	2.97	3.10±0.14
197.97	0.450	0.738	2.82	2.84±0.12
307.68	0.690	0.825	1.99	1.86±0.11

Table 6
Order of reflection $n = 3$ ($F = 14.52$).

E[keV]	$\bar{f}(A_m)$	$\exp(-\bar{g} \cdot \bar{Q}' t_\theta)$	$R_{th} \cdot 10^6$	$R_{obs} \cdot 10^6$
63.12	0.584	0.914	2.76	2.76±0.14
109.77	0.571	0.586	2.73	2.72±0.13
130.51	0.569	0.685	2.25	2.21±0.11
177.18	0.567	0.815	1.45	1.47±0.07
197.97	0.556	0.849	1.21	1.21±0.05
307.68	0.706	0.919	0.68	0.68±0.03

7. Conclusion

Inspection of the values in Tables 4–6 shows that the observed reflectivities are accurately reproduced by the introduction of a transverse dimension t_t. This also eleminates the systematic decrease of t_m with increasing diffraction order. But the parameters are not equal at all three orders. If we compute the mean value for each parameter, we obtain:

$$\overline{t_m} = 0.60 \text{ mm} \qquad \overline{t_t} = 0.02 \text{ mm} \qquad \overline{(\bar{g})} = 9.10 \cdot 10^4$$

The value for $\overline{t_m}$ is about the same as that obtained for the 2.5 mm plate. This is expected since both plates were cut from the same crystal.

The mosaic width corresponding to $\overline{(\bar{g})} = 9.1 \cdot 10^4$ is about 1.8 arcsec. The increase in this value is reflected in the observed width of the reflexes which is 4.5 arcsec for the 6 mm plate, and 3.5 arcsec for the 2.5 mm thick plate.

A striking difference was noted between the dimensions $\overline{t_m}$ and $\overline{t_t}$. It is too large to be attributed to intrinsic anisotropies with respect to a growth direction. We believe rather that is an effect of bending and/or bending imperfections. This hypothesis could possibly be verified by the determination of the parameters $\overline{t_m}$ and $\overline{t_t}$ as a function of bending radius.

Acknowledgements

We express our gratitude to Drs R. D. Deslattes, A. Burek and W. Schwitz of the U.S. National Bureau of Standards for their helpful remarks and suggestions. We would like to thank Prof. O. Huber for his constant interest. We acknowledge thankfully the help of H. Tschopp and of Ch. Rhême in the development of the measuring apparatus.

REFERENCES

[1] O. I. SUMBAYEV, Soviet. Phys. JEPT *5*, 1042 (1957).
[2] W. BEER and J. KERN, Nucl. Instr. and Meth. *117*, 183 (1974).
[3] J.-Cl. DOUSSE and J. KERN, phys. Letters *59A*, 159 (1976) and Acta Cryst. *36A* (1980), in press.
[4] J. W. M. DUMOND, Rev. Sci. Instr. *18*, 626 (1947).
[5] R. W. JAMES, *The Optical Principles of the Diffraction of X-Rays*, ed. by L. BRAGG, London: Bell & Sons Ltd, p. 51 (1967).
[6] W. ZACHARIASEN, *Theory of X-Ray Diffraction*, New York: J. Wiley & Sons, Inc., p. 128 & pp. 168–169 (1946).
[7] Y. CAUCHOIS and C. BONNELLE, *Atomic Inner Shell Processes*, Vol. II, New York: Academic Press, p. 103 (1975).
[8] C. G. DARWIN, Phil. Mag. 27, p. 315 & p. 675 (1914).
[9] C. G. DARWIN, Phil. Mag. *43*, 800 (1922).
[10] L. V. AZÁROFF, *Elements of X-Ray Crystallography*, New York: McGraw-Hill Book Company, p. 212 (1968).
[11] R. D. DESLATTES and B. PARETZKIN, J. Appl. Cryst. *1*, 176 (1968).
[12] J. DESPUJOLS, *Symp. on Cryst. Diffr. of Nucl. Gamma-Rays*, edited by F. BOEHM, Calif. Inst. of Technology, Pasadena p. 194 (1964).
[13] J.E. WHITE, J. App. Phys. *21*, 855 (1950).